High Resolution Electron Microscopy and X-Ray Powder Diffraction Studies of $Sr_2Nb_5O_9$

Gunnar Svensson

Department of Inorganic Chemistry, Arrhenius Laboratory, University of Stockholm, S-106 91 Stockholm, Sweden

Svensson, G., 1990. High Resolution Electron Microscopy and X-Ray Powder Diffraction Studies of $Sr_2Nb_5O_9$. – Acta Chem. Scand. 44: 222–227.

A new reduced strontium niobate, $Sr_2Nb_5O_9$, has been found. The space group is $P4/mmm$ and its unit cell parameters are a = 4.1405(2) and c = 12.040(2) Å. It is isostructural with $Ba_2Nb_5O_9$, having alternating slabs of $SrNbO_3$ (perovskite) and NbO. In the NbO layer Nb_6 octahedra are vertex-linked in two dimensions, having Nb–Nb bonds. The structure has been confirmed by comparing observed and calculated X-ray powder diffraction patterns. HREM studies have shown the presence of defects, where the layers have broken up to form a disordered intergrowth between NbO and $SrNbO_3$ blocks.

In the reduced part of the Sr–Nb–O system, the following phases have been known for some time, namely Sr_xNbO_3,[1] $Sr_5Nb_5O_{16}$[2] and $Sr_7Nb_6O_{21}$.[3] Recently $SrNb_8O_{14}$[4] was found, together with two new reduced phases in the Ba–Nb–O system, $Ba_2Nb_5O_9$[5] and $BaNb_8O_{14}$.[6] The structure of $Ba_2Nb_5O_9$ was found to be an ordered intergrowth of alternating layers of the perovskite type ($BaNbO_3$)[7] and an ordered deficient NaCl-type structure (NbO).[8] The NbO layer consists of Nb_6 octahedra sharing corners in two dimensions, with metal–metal bonds between the Nb atoms. It can also be described as comprising condensed Nb_6O_{12} clusters.[9] The Nb_6 octahedra in such a cluster can be coordinated by oxygen atoms according to the scheme $Nb_6O^i_{12}O^a_6$ (Fig. 1a). There are 12 oxygen atoms outside the edges (O^i) and 6 located outside the apices (O^a) of the Nb_6 octahedra. This notation can also be used to describe the connection pattern between octahedral clusters, see e.g. Ref. 10. Some examples of linkage are shown in Fig. 1b.

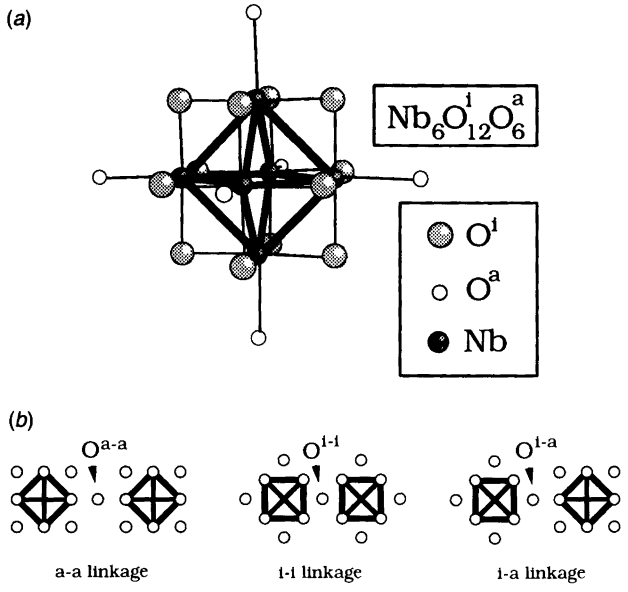

Fig. 1. (*a*) A $Nb_6O^i_{12}O^a_6$ cluster showing the O^i and O^a atoms. The former are located outside the edges, bonded to two Nb atoms in the same cluster, the latter outside the apices, bonded only to one Nb in the cluster. (*b*) Examples of inter-cluster connection, $O^{i\text{-}i}$, $O^{a\text{-}a}$ and $O^{i\text{-}a}$ linkage.

When the compositions are moved towards the NbO–Nb_2O_5 binary line of the phase diagram, the NbO layers in $Ba_2Nb_5O_9$ break up. Instead, blocks of corner-sharing Nb_6 octahedra in a perovskite ($BaNbO_3$) matrix form.

Since a perovskite-type phase corresponding to $BaNbO_3$ also exists in the Sr–Nb–O system, it was natural to investigate if an $Sr_2Nb_5O_9$ phase, isostructural with $Ba_2Nb_5O_9$, could be prepared. It was also interesting to see if block structures similar to those found in the Ba–Nb–O system could be prepared. This paper will discuss the stoichiometric $Sr_2Nb_5O_9$ phase and also briefly the defects found in it.

Experimental

The starting materials used for the preparation were Nb_2O_5 (puriss, 99.9 %, Roth Co.; purified of oxide-fluorides by heating in air at 1100 °C), Nb (400 mesh), and $Sr_5Nb_4O_{15}$.[11–13] This latter phase was obtained by heating appropriate amounts $SrCO_3$ (Baker's analysed) at 1000 °C for 24 h, then regrinding and heating again at 1100 °C for a further 18 h. The phase composition of the product was checked by means of X-ray powder diffraction patterns. Appropriate amounts of $Sr_5Nb_4O_{15}$, Nb and Nb_2O_5 were ground and pelleted in order to minimise the reaction with the walls of the silica tube. These tubes were evacuated and sealed. Temperatures from 1100 to 1250 °C for 1–2 days were normally used, but longer periods were also tested. The tubes were air-quenched. The surfaces of the tablets

were always coated by a silicon-containing product which was removed mechanically. X-Ray powder diffraction patterns were taken in a focusing camera of the Guinier–Hägg type, using Cu $K\alpha_1$ radiation. Silicon [a = 5.430880(35) Å][14] was added as internal standard. The films were analysed with a film scanner system.[15] The unit cell parameters of $Sr_2Nb_5O_9$ were refined with the program PIRUM.[16]

Electron microscopy studies were made at 200 kV in a Jeol 200CX instrument. The structure model of $Sr_2Nb_5O_9$ was tested by image calculation according to the multislice method using a local version of the program suite SHRLI[17] and by comparing observed and calculated X-ray powder diffraction patterns.

Results

In the reduced part of the SrO–NbO–Nb_2O_5 system preparations corresponding to Sr_xNbO_3, $Sr_2Nb_5O_9$, $SrNb_8O_{14}$ and some intermediate compositions were made.

Sr_xNbO_3 was reported by Ridgley and Ward[1] to have a perovskite type structure. They found that the Sr content x varied from 0.7 to 0.95 and that the unit cell dimension obeyed Vegard's law. $Sr_{0.7}NbO_3$ had a = 3.981 Å, while $SrNbO_3$ had a = 4.020 Å. We also observed varying cell dimensions. A sample with the nominal composition $Sr_{1.1}NbO_3$ (I) (synthesised at 1100 °C) had a = 4.0216(2) Å, while in a polyphasic sample with the gross composition $Sr_2Nb_{5.1}O_{8.8}$ (II) (synthesised at 1200 °C) the lattice parameter was a = 3.9951(1) Å. In the X-ray powder pattern of sample (I) there were some unidentified lines besides those from $SrNbO_3$, and in (II) lines from NbO and $Sr_2Nb_5O_9$ were also seen.

$Sr_2Nb_5O_9$ formed only at temperatures at or above 1200 °C. Below this temperature only lines corresponding to Sr_xNbO_3 and NbO were found in the powder patterns. At these high temperatures and prevailing reducing conditions the SiO vapour pressure in the silica tubes is high, and silicon-containing products form on the surface of the pellets upon prolonged heating. This decreases the amount of Sr available for the formation of strontium niobates. In the X-ray pattern of a sample with the nominal composition $Sr_2Nb_{5.1}O_{8.8}$ heated at 1250 °C for 3 weeks, only Sr-poor phases such as $SrNb_8O_{14}$, NbO and α (see below) were observed. Monophasic samples of $Sr_2Nb_5O_9$ were never obtained. There were always strong lines from both Sr_xNbO_3 present. In most cases $Sr_2Nb_5O_9$ was the minor phase. Regrinding and reannealing did not increase the amount of $Sr_2Nb_5O_9$. Once the reflections corresponding to $SrNbO_3$ and NbO in the diffraction pattern had been removed, all the remaining lines were found to correspond to $Sr_2Nb_5O_9$, and a least-squares refinement yielded the unit cell parameters a = 4.1405(4) and c = 12.040(2) Å. The observed and calculated d-values are given in Table 1.

To investigate a possible disordered intergrowth between blocks of NbO and perovskite-type blocks, similar to that found in the Ba system,[18] a synthesis with the composition $SrNb_6O_8$ at 1200 °C was made. This composition is on the two-phase line between $Sr_2Nb_5O_9$ and NbO. In the corresponding X-ray powder diffraction pattern we found lines from NbO (strong),[8] $SrNb_8O_{14}$ (weak),[4] Sr_xNbO_3 (weak)[1] and the $hk0$ reflections from $Sr_2Nb_5O_9$ (strong). The position of these last lines were slightly shifted compared to $Sr_2Nb_5O_9$. There were also some new reflections. In the Ba

Table 1. Observed and calculated d-values and X-ray powder intensities for $Sr_2Nb_5O_9$.

hkl	d_{obs}/Å	I_{rel}	d_{calc}/Å	I_{calc}
001	12.11	9	12.04	16
002	6.02	3	6.02	7
100	4.141	9	4.141	13
003			4.013	<1
101	3.921	1	3.916	8
102	3.411	2	3.412	2
004	3.011	3	3.011	3
110	2.927	13	2.928	15
103	2.882	100	2.882	100
111	2.843	55	2.845	57
112	2.632	34	2.633	39
104			2.435	2
005	2.407	1	2.408	1
113	2.365	13	2.365	12
114	2.099	19	2.099	16
105			2.082	4
200	2.070	82	2.070	75
201	2.040	2	2.040	1
006	2.005	42	2.007	34
202	1.958	3	1.958	1
115	1.860	17	1.860	16
210	1.852	4	1.852	3
203			1.840	<1
211			1.830	2
106	1.806	3	1.806	3
212	1.771	2	1.770	1
007			1.720	<1
204	1.706	2	1.706	3
213	1.681	65	1.681	47
116	1.655	7	1.655	7
107			1.584	<1
214			1.577	1
205	1.570	3	1.570	1
008			1.505	<1
117	1.483	7	1.483	10
215			1.468	3
220	1.464	36	1.464	27
221			1.453	<1
206	1.441	69	1.441	52
222	1.422	2	1.422	1
108			1.414	<1
300			1.380	1
223			1.375	<1
301			1.371	1
216	1.361	3	1.361	2
302			1.345	<1
118	1.339	6	1.339	8
009			1.338	<1
207			1.323	<1
224			1.316	1
310	1.309	5	1.309	4
303	1.305	18	1.305	13

system[18] a sample with a similar composition gave an X-ray pattern having lines from NbO and the *hk*0 reflections from $Ba_2Nb_5O_9$, together with some new ones. The more intense of these new reflections and those at positions corresponding to the *hk*0 lines of $Ba_2Nb_5O_9$ could be indexed on the basis of a tetragonal lattice, having the unit cell axes a = 4.164(1) and c = 4.151(1) Å.[18,19] This "phase" was called A_{def}, but here it will be called α. Such a cell was also found here, having the axes a = 4.120(1) and c = 4.141(1) Å. After the lines corresponding to this cell had been indexed only two weak reflections remained unidentified in the powder pattern. The α "phase" in the barium system corresponds to a two- (three-) dimensional intergrowth of NbO in $BaNbO_3$.[18,19] This is briefly discussed below.

Structure. The similarity in unit cell dimensions and composition between $Sr_2Nb_5O_9$ and $Ba_2Nb_5O_9$[5] made it reasonable to assume that they were isostructural. The atomic coordinates for $Ba_2Nb_5O_9$ (slightly shifted) and space group *P*4/mmm, together with the unit cell obtained for $Sr_2Nb_5O_9$, were used to calculate an X-ray powder diffraction pattern for $Sr_2Nb_5O_9$. In this model the following assumptions were made; (1) the Nb_6 octahedra are given cubic symmetry, with their size determined by the length of the *a*-axis, and (2) the Sr positions are fully occupied. The atomic coordinates used for the calculated X-ray powder diffraction pattern and the simulated lattice images are given in Table 2. As seen in Table 1, only minor differences exist between the observed and calculated intensities. The observed X-ray pattern corresponds to a sample with the nominal composition $Sr_2Nb_{5.1}O_{8.8}$. The intensities in Table 1 were used to calculate $R_I = \Sigma|I_{obs}-I_{cal}|/I_{obs}$ = 18 %. The model was not refined, since there were relatively strong reflections from both $SrNbO_3$ and NbO present in the diffraction patterns which affect the line profiles.

Analogous to $Ba_2Nb_5O_9$, the structure is built up from alternating layers of $SrNbO_3$ (perovskite) and NbO (ordered deficient NaCl), Fig. 2. The perovskite layers are two unit cells, and the NbO layers one unit cell thick, having boundary atoms in common. The bond lengths are reasonable and similar to those found in $Ba_2Nb_5O_9$. The Nb_6O_{12} clusters in the NbO layer have Nb–Nb bond lengths of 2.928 Å. This is slightly shorter than the value of 2.948 Å in $Ba_2Nb_5O_9$. A more thorough description of that structure has been given in Ref. 5.

Table 2. Atomic coordinates for $Sr_2Nb_5O_9$ used for calculated X-ray powder diffraction pattern and lattice image simulations.[a]

Atom	*x*	*y*	*z*
Sr	0.0	0.0	0.1694
Nb(1)	0.0	0.5	0.5
Nb(2)	0.5	0.5	0.3280
Nb(3)	0.5	0.5	0.0
O(1)	0.5	0.0	0.0
O(2)	0.5	0.5	0.165
O(3)	0.5	0.0	0.329
O(4)	0.0	0.0	0.5

[a]Space group *P*4/mmm; a = 4.1405(4), c = 12.040(2) Å; V = 206.41 Å^3.

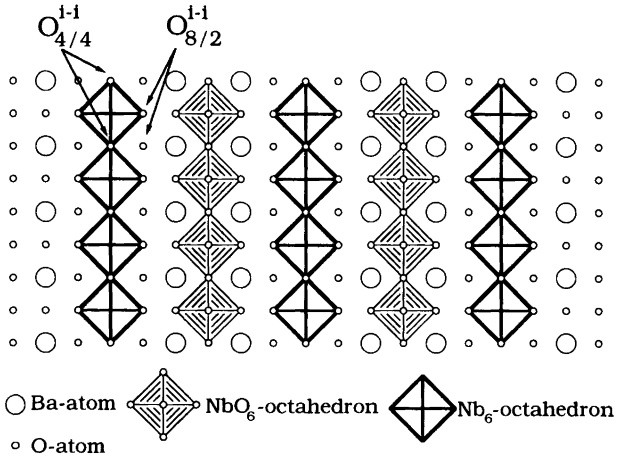

Fig. 2. An idealized structure model of $Sr_2Nb_5O_9$, viewed along the *a*-axis. The Nb–Nb bonds in the Nb_6 octahedra in the single NbO layer are heavily outlined. Note that there are –Nb–O–Nb–O chains projecting below all outer corners of the Nb_6 octahedra; only the oxygen atoms are shown. The double perovskite layer consists of one whole and two half NbO_6 octahedra and shares half of its niobium atoms with the NbO layer. In the model only the complete NbO_6 octahedra are outlined. The connection pattern of the O^i atoms in the clusters is marked.

High-resolution electron microscopy. A lattice image of a $Sr_2Nb_5O_9$ crystal taken along ⟨100⟩ is shown in Fig. 3. The image can be described as a square net of dark spots 2.9 Å apart. Diagonally to this net, dark rows are seen separated by ca. 12 Å. The square net corresponds to Sr and the Nb

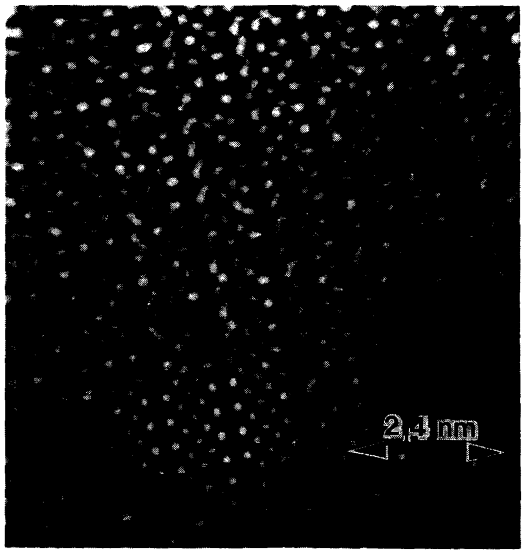

Fig. 3. HREM image of $Sr_2Nb_5O_9$ viewed along the *a*-axis. In the image a calculated image has been inserted (defocus −600 Å, objective aperture size 0.41 Å^{-1}, thickness 21 Å).

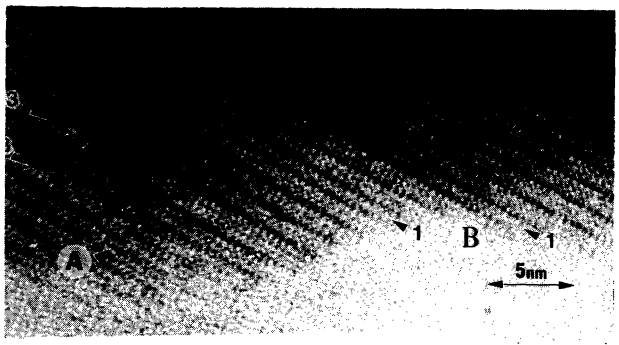

Fig. 4. HREM image of a crystal found in a sample with the nominal composition $Sr_2Nb_5O_{8.8}$. The main part of the crystal is stoichiometric $Sr_2Nb_5O_9$, but in the region shown there are some defects. There are perovskite slabs having an extra layer of octahedra (arrows marked 3) and those with one layer missing (arrows marked 1). In connection with the wider perovskite slabs an area (A) with more complicated defects is seen. The structure is shifted along the *c*-axis twice. In connection with this a 2×2 block of dark contrast is found, corresponding to 2×2 corner-sharing Nb_6 octahedra. In one of the dark rows one dark spot is missing which should correspond to a missing projected column of Nb_6 octahedra. Tentative models of the areas marked A and B are shown in Figs. 5a and 5b.

atoms in the perovskite layer, and the dark rows to the Nb atoms in NbO layers in $Sr_2Nb_5O_9$. Note that at this degree of defocusing there is no significant difference in contrast between the Sr and Nb atoms in the perovskite layer. A simulated image of $Sr_2Nb_5O_9$ has been inserted into the image. The agreement between observed and simulated images is reasonable.

In the same sample, the crystal shown in Fig. 4 was found. The main part of this crystal consists of stoichiometric $Sr_2Nb_5O_9$, but in the region shown defects are present. Perovskite-type slabs of smaller as well as larger spacing compared to $Sr_2Nb_5O_9$ are seen, indicated by the arrows marked 1 and 3, respectively. In one part of the defect, the dark rows corresponding to NbO layers are shifted by *c*/2, and are shifted back after ca. 16 Å. In connection with these shifts, a more disordered region is present, marked A.

Tentative models of the defects marked A and B in the lattice image are shown in Figs. 5a and 5b, respectively. In the region interpreted, it is assumed that the structural elements extend through the whole thickness of the crystal. The bonding distances in the models are all in the same range as found in $Sr_2Nb_5O_9$. The defects with thinner (denoted 1) and wider (denoted 3) perovskite-type slabs represent homologues with a missing and an extra $SrNbO_3$ octahedral layer, respectively. The thin slabs consist of only a single perovskite unit. In the image shown, there are two such thin layers separated by two "normal" $Sr_2Nb_5O_9$ layers. These thin slabs share all their niobium atoms with the adjacent NbO layers (Fig. 5b). Alternatively they can be described as single SrO layers between NbO layers. The similarity in scattering power of Sr and Nb makes it hard to say if the dark spots in the perovskite slabs correspond to Sr or Nb atoms. A simple charge balance calculation gives no definite answer. However, since no Nb–O binary phase containing both Nb_6O_{12} clusters and NbO_6 octahedra is known, it seems more reasonable to assume that the layers consist of SrO. As stated above, there is a more disordered region A in connection with the defects with wider perovskite slabs (arrowed 3 in Fig. 4). There are also other types of defects found. Parts of this area are hard to interpret unequivocally, but a tentative model is shown in Fig. 5a.

In the same crystal, areas where the alternating slabs of NbO and perovskite types have locally broken up were also found. Then there are isolated NbO blocks of corner-sharing Nb_6 octahedra. These blocks are of the same type as reported for the barium system in Refs. 18 and 19. An example is shown in Fig. 6, together with a tentative model of the image. In this model the perovskite parts between the NbO blocks have been arranged so as to maximize the number of Sr atoms.

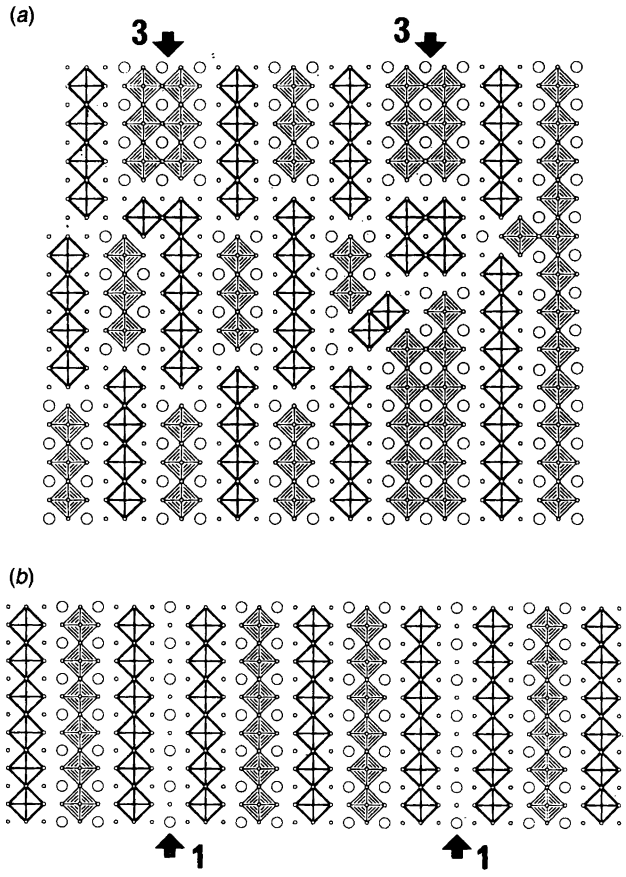

Fig. 5. Tentative models of the regions marked A and B in the HREM image shown in Fig. 4. The Nb_6 octahedra in the Nb_6O_{12} cluster are heavily outlined. (*a*) This model shows a region (A) with more complicated defects. The extra wide perovskite layers (arrows marked 3) are unequivocally interpreted, but the other defect models are more tentative, since it is impossible to distinguish between Sr and Nb at this defocus. (*b*) The defect (B) with a single perovskite layer (arrows marked 1 in Fig. 4). In the perovskite layer all remaining Nb atoms are shared with the NbO layer. This single layer can also be described as an SrO layer inserted between layers of condensed Nb_6O_{12} clusters.

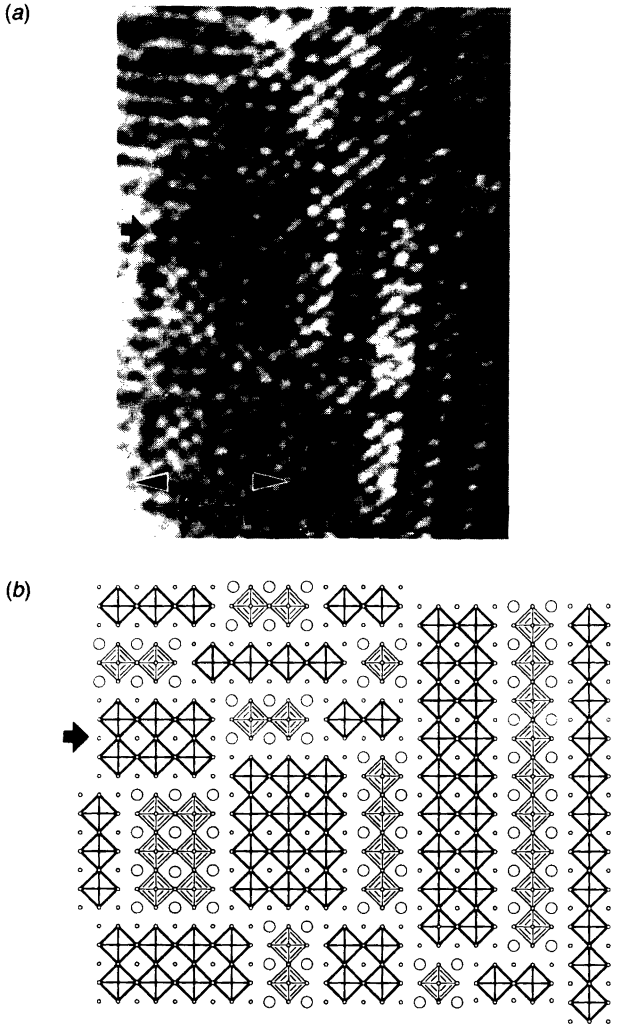

Fig. 6. (*a*) A lattice image of an area found in the same crystal as shown in Fig. 4. It can be described as blocks of dark spots separated by 4 Å. Between these blocks are areas with lighter contrast separated by 2.9 Å. The blocks can be interpreted as consisting of corner-sharing Nb_6 octahedra (or $NbO–Nb_6O_{12}$ clusters), inserted in a perovskite lattice, ($SrNbO_3$). (*b*) A tentative model of a part of the image. The perovskite blocks between the NbO blocks are independently oriented so as to maximize the amount of Sr. The arrows highlight the same NbO block in the image and in the model.

As described in Ref. 18, a shift of the composition of the samples towards the $NbO–Nb_2O_5$ binary line in the phase diagram of the $BaO–NbO–Nb_2O_5$ system increases the number of block structure crystals. In the sample of composition $SrNb_6O_8$ discussed above, several such crystals were found. This type of intergrowth will be discussed in some detail elsewhere.[19]

Discussion

The unit cell of $Sr_2Nb_5O_9$ is slightly smaller than that of $Ba_2Nb_5O_9$. This difference reflects the smaller size of the unit cell of $SrNbO_3$ compared to $BaNbO_3$. The size difference between $BaNbO_3$ and NbO is quite small. When forming $Ba_2Nb_5O_9$, an intergrowth of these structures, the $BaNbO_3$ parts have expanded by 1.02 % and NbO has decreased by 0.97 %. $SrNbO_3$ is smaller than $BaNbO_3$, and consequently the size difference between $SrNbO_3$ and NbO is larger, 4.5 %. It is mainly the *c*-axis in $Sr_2Nb_5O_9$ that has shrunk in comparison with that in $Ba_2Nb_5O_9$. The shortening along the *a*-axis in $Sr_2Nb_5O_9$ is limited by the size of the Nb_6 octahedra, which may act as a framework, obstructing a full decrease in length. The *c*-axis is not affected by this constraint, and can therefore shrink freely.

The frequency of defects in "stoichiometric" $Sr_2Nb_5O_9$ crystals was higher than in $Ba_2Nb_5O_9$, as found in HREM studies.

The two defect types, with thinner and wider perovskite layers between the NbO slabs, can be considered as being members with $n = 1$ and 3, respectively, of a homologous series $Sr_nNb_{3+n}O_{3+n}$. Defects representing the same members, as well as some with higher *n*-values, have been observed in the Ba system. No ordered homologues have been found, however.

It is interesting to compare this structure with the one obtained for $SrNb_8O_{14}$ by Köhler *et al.*[4] That structure also contains NbO_6 octahedra and Nb_6O_{12} clusters. In contrast to $Sr_2Nb_5O_9$, it has discrete metal clusters, which are connected via oxygen atoms, forming chains. The connection pattern is $[Nb_6O^{i-i}_{2/2}O^{i}_{8}O^{i-a}_{2}]O^{a-i}_{2}O^{a-a}_{4/2}$, while in $Sr_2Nb_5O_9$ it is $Sr_2Nb_5O_9$ = "$Sr_2NbO_2 \cdot Nb_4O_7$" = "$Sr_2NbO_2 \cdot Nb_2Nb_{4/2}O^{i-i}_{4/2}O^{i-i}_{8/2}O^{a}_{2}$". The $O^{i-i}_{4/4}$ and $O^{i-i}_{8/2}$ atoms are marked in Fig. 2.

A simple charge-balance calculation gives the oxidation number +4 for Nb(3) in the $Sr_2Nb_5O_9$ perovskite layer. Then the number of electrons involved in metal–metal bonding in the cluster is 10 per unit cell, which is close to the 9 per unit cell found in NbO. This is also reflected in the similarity of the Nb–Nb bond lengths, 2.93 Å in $Sr_2Nb_5O_9$ and 2.97 Å in NbO. This number of electrons should be compared with the value of 14–16 found in structures having discrete clusters, e.g. $SrNb_8O_{14}$,[4] $Mg_3Nb_6O_{11}$,[20,21] $Mn_3Nb_6O_{11}$,[21] $NaNb_{10}O_{18}$[22] and $BaNb_8O_{14}$[6] have 14, $Na(Si,Nb)Nb_{10}O_{19}$[23] has 14.33, $Na_3Al_2Nb_{34}O_{64}$[23] has 15 and $Na(V_{3-x}Nb_x)Nb_6O_{12}$[24] has 16.

Acknowledgements. I wish to thank Professor L. Kihlborg for many stimulating and helpful discussions. This work is part of a research project supported by the Swedish Natural Science Research Council.

References

1. Ridgley, D. and Ward, R. *J. Am. Chem. Soc. 77* (1955) 6132.
2. Schückel, K. and Müller-Buschbaum, H. *Z. Anorg. Allg. Chem. 528* (1985) 91.
3. Schückel, K. and Müller-Buschbaum, H. *Z. Anorg. Allg. Chem. 523* (1985) 89.
4. Köhler, J., Simon, A., Hibble, S. J. and Cheetham, A. K. *J. Less-Common Met. 142* (1988) 123.
5. Svensson, G. *Mater. Res. Bull. 23* (1988) 437.
6. Hibble, J. S., Cheetham, A. K., Köhler, J. and Simon, A. *Eur. J. Inorg. Solid State Chem. Submitted.*
7. Kreiser, R. and Ward, R. *J. Solid State Chem. 1* (1970) 368.
8. Andersson, G. and Magnéli, A. *Acta Chem. Scand. 11* (1957) 1065.
9. Schäfer, H. and Schnering, H. G. *Angew. Chem. 20* (1964) 833.
10. Simon, A. *Angew. Chem., Int. Ed. Engl. 27* (1988) 159.
11. Spitsyn, V. I., Ippolitov, E. A., Kovna, L. M., Lykova, L. N. and Leschenkov, P. P. *Russ. J. Inorg. Chem. 27* (1982) 464.
12. Appendino, P. and Burlando, G. A. *Atti Accad. Sci. Torino 197* (1973) 97.
13. Whiston, C. D. and Smith, A. J. *Acta Crystallogr. 23* (1967) 82.
14. Hubbard, C. R., Swanson, H. E. and Mauer, F. A. *J. Appl. Crystallogr. 8* (1975) 45.
15. Johansson, K.-E., Palm, T. and Werner, P.-E. *J. Phys. E 13* (1980) 1289.
16. Werner, P.-E. *Ark. Kemi 31* (1969) 513.
17. O'Keeffe, M. A. In: Hren, J. J., Lenz, F. A., Munro, E. and Sewer, P. B., Eds., *Electron Optical System for Microscopy, Microanalysis and Microlithography, (Proc. 3rd Pfeffercorn Conf.)* SEM Inc., AMF O'Hare, IL 60666, U.S.A. 1984.
18. Svensson, G. *Solid State Ionics 32/33* (1989) 126.
19. Svensson, G. *Chem. Commun. Univ. Stockholm 3* (1989).
20. Marinder, B.-O. *Chem. Scr. 11* (1977) 97.
21. Burnus, R., Köhler, J. and Simon, A. *Z. Naturforsch. B 42* (1987) 536.
22. Köhler, J. and Simon, A. *Z. Anorg. Allg. Chem. In press.*
23. Köhler, J. and Simon, A. *Z. Anorg. Allg. Chem. 553* (1987) 106.
24. Köhler, J., Miller, G. and Simon, A. *Z. Anorg. Allg. Chem. 568* (1989) 8.

Received June 9, 1989.